Effect of metabolic uncoupler, 2, 4-dinitrophenol (DNP) on sludge properties and fouling potential in ultrafiltration membraneprocess

An Ding[a], Dachao Lin[a], Yingxue Zhao[a], Huu Hao Ngo[b], Wenshan Guo[b],

*Langming Bai[a], Xinsheng Luo[a], Guibai Li[a], Nanqi Ren[a], Heng Liang[*a]*

[a] *State Key Laboratory of Urban Water Resource and Environment (SKLUWRE), School of Environment, Harbin Institute of Technology, 73 Huanghe Road, Nangang District, Harbin, 150090, P.R. China*

[b] *Faculty of Engineering, University of Technology Sydney, P.O. Box 123, Broadway, Sydney, NSW 2007, Australia*

(dinganhit@163.com; 455141870@qq.com; 503275242@qq.com; haon@eng.uts.edu.au; wenshan.guo-1@uts.edu.au; andy_white@126.com; 247138574@qq.com; liguibai@vip.163.com; rnq@hit.edu.cn; hitliangheng@163.com)

* Corresponding author: Heng Liang, hitliangheng@163.com

Abstract

Energy uncoupling technology was applied to the membrane process to control the problem of bio-fouling. Different dosages of uncoupler (2, 4-dinitrophenol, DNP) were added to the activated sludge, and a short-term ultrafiltration test was systematically investigated for analyzing membrane fouling potential and underlying mechanisms. Ultrafiltration membrane was used and made of polyether-sulfone with a molecular weight cut off (MWCO) of 150 kDa. Results indicated that low DNP concentration (15-30 mg/g VSS) aggravated membrane fouling because more soluble microbial products were released and then rejected by the membrane, which significantly increased cake layer resistance compared with the control. Conversely, a high dosage of DNP (45 mg/g VSS) retarded membrane fouling owing to the high inhibition of extracellular polymeric substances (proteins and polysaccharides) of the sludge, which effectively prevented the formation of cake layer on the membrane surface. Furthermore, analyses of fouling model revealed that a high dosage of DNP delayed the fouling model from pore blocking transition to cake filtration, whereas this transition process was accelerated in the low dosage scenario.

Key words: Energy uncoupling; Bio-fouling; Sludge property; Filtration resistance; Fouling model; Extracellular polymeric substance (EPS)

1. Introduction

Due to the high quality of the permeate, complete biomass retention and small footprint, membrane bioreactors (MBRs) now constitute a widely implemented wastewater treatment technology combining an activated sludge process and membrane filtration. However, membrane fouling remains in most cases and this issue continues to increase operation costs and reduce the quantity of water (Malaeb et al., 2013). Of all the types of fouling, bio-fouling is one of the most serious operational problems in membrane applications. Bio-fouling is defined as the undesirable accumulation of microorganisms at a phase transition interface (solid-liquid, gas-liquid or liquid-liquid), which may occur through deposition, growth and metabolism of bacteria cells or flocs on the membrane surface. Therefore, conventional physical cleaning processes such as back-washing and back-pulsing are no longer effective.

Recently, biological-based anti-fouling strategies, for instance quorum quenching, enzymatic disruption, cell wall hydrolysis and energy uncoupling have begun to prove their potential as more viable solutions than conventional control methods, based on engineering, material, and chemical principles (Malaeb et al., 2013). Among these strategies, energy uncoupling technology is relatively easy to implement by adding metabolic uncouplers, and via the addition of these chemicals can transport protons through the cellular membrane. In this proton gradient is dissipated and adenosine triphosphate (ATP) synthesis inhibited (Liu, 2000).

Xu and Liu (2011) have produced evidence of suppressed ATP synthesis and autoinducer-2 (AI-2) production using 2, 4-dinitrophenol (DNP) to remove biofilm bacteria from nylon membrane surfaces. Membrane bio-fouling could be controlled through the inhibition of ATP synthesis, which was made possible by chemical uncoupling for the off-line membrane cleaning process. A possible explanation for this is that the addition of DNP reduced the biofilm's extracellular polymeric substance (EPS) contents. Several researchers have confirmed that ATP synthesis and AI-2 of the biomass were inhibited by the addition of 3, 3', 4', 5-tetrachlorosalicylanilide (TCS), thereby reducing the production of EPS contents. As a result,

granular sludge biofilm could not form and even appeared in a disorganized state (Jiang & Liu, 2010; Xiong & Liu, 2010). Li et al. (2012) studied the effect of TCS on the soluble microbial products (SMP) production of activated sludge, and discovered that the addition of TCS in activated sludge system led to an increased production of SMP, especially proteins. The increased SMP production was associated with substrate utilization at a low TCS concentration, while more non-substrate-associated SMP was released at a high TCS concentration.

It is well known that EPS in either bound or soluble form (correspond to SMP) are currently considered as the predominant cause of membrane fouling in MBRs (Meng et al., 2017). EPSs can block membrane pores, attach to membrane surface, influence cake structure and induce osmotic effect, showing profound impacts on membrane fouling. The extracted EPSs alone had a specific filtration resistance, which was 1000 times higher than the sludge flocs. EPSs can be regarded as material base or medium of membrane fouling process in MBRs, through which, other foulants directly or indirectly take roles in membrane fouling. (Lin et al., 2014). Investigations have revealed that EPSs produced by the deposited microbial cells becomes a major foulant after the trans-membrane pressure (TMP) jump. In contrast, the SMP compounds play an important role in the initial fouling (Zhou et al., 2015). Additionally, initial adhesion of SMP and biopolymers colonized membrane surface, and then facilitated the following adhesion of sludge flocs and EPS (Wang et al., 2013).

Based on the literature, it can be expected that the addition of uncouplers (DNP) to the MBR process might change the physicochemical properties of activated sludge (especially EPS and SMP), and further influence the membrane fouling potential. To the best of our knowledge, limited attention has been paid to these issues. To this end, the aims of this study were therefore to: (1) evaluate the effect of different dosages of DNP on the properties of the sludge; (2) explore the optimal dosage for alleviation of bio-fouling; (3) analyze the distribution of filtration resistance and fouling models; and (4) elucidate the mechanisms of energy uncoupling for bio-fouling control.

2. Materials and methods

2.1 Sludge samples and dead-end ultrafiltration (UF) test

The activated sludge used for experiments was collected from Wenchang wastewater treatment plant in Harbin, China. Different dosages of DNP with the values of 0 mg/g VSS, 15 mg/g VSS, 30 mg/g VSS and 45 mg/g VSS were added to the activated sludge, and the samples were named S1, S2, S3 and S4, respectively. All the samples were cultured at room temperature (25 °C) for 24 hours. In addition, the concentration of dissolved oxygen in all the samples was controlled at 4 mg/L. Magnetic stirrers were used for mixing the sludge, and the rotate speed was 50 rpm. After that, the sludge samples were collected from different groups for measurements.

To understand the membrane fouling potential and mechanisms, dead-end UF tests were used to investigate the initial stage of membrane filtration, which could help in the development of fouling mitigation strategies in the MBR process (Ding et al., 2015; Shen et al., 2010). The experiments were conducted in a filtration cell (Amicon 8400, Millipore, USA) under dead-end mode without any stirring at room temperature (25 °C). During the filtration, flat sheet polyether-sulfone (PES) UF membrane with an MWCO of 150 kDa was placed on the bottom of the cell with the glossy side facing the feed solution. The effective filtration surface area was 43 cm^2. The maximum volume of the membrane cell was 350 mL and pressure was maintained using nitrogen gas at 30 kPa. The weight of the permeate was recorded automatically every five seconds.

2.2 Resistances-in-series model

To evaluate the fouling behavior, Darcy's law was applied to calculate the total fouling resistance as shown in Eq. (1):

$$J = \frac{\Delta P}{\mu R_t} \qquad (1)$$

$$R_t = R_m + R_p + R_c \qquad (2)$$

where J is permeate flux (m^3 m^{-2} s^{-1}), ΔP is trans-membrane pressure (Pa), μ is dynamic viscosity (Pa·s), and R represents resistance (m^{-1}). As shown in Eq. 2, total resistance (R_t) consists of the resistance of the membrane (R_m), resistance of the pore blocking (R_p) and resistance of the cake layer (R_c). R_m was determined by measuring the flux of de-ionized water (DI) with a clean membrane. R_c was determined based on the difference in the overall resistance before and after the cake layer was cleaned using a sponge. Finally, R_p was calculated by extracting R_m and R_c from R_t.

2.3 Modelling of flux decline with membrane-blocking mechanisms

The flux decline of UF in the dead-end cell under constant pressure can be described by different blocking mechanisms, as follows: complete blocking, standard blocking, intermediate blocking and cake filtration. The details concerning this method can be found in Shen et al. (Shen et al., 2010).

2.4 Analytical methods

2.4.1 SMP and EPS

The SMP was obtained by centrifuging the sludge at 4000 rpm for 10 min, and then filtering through a 0.45 μm membrane. Extraction of the EPS from the sludge was conducted by the heating method as described by Adav and Lee (2008). The quantification of protein in SMP (SMP$_{pr}$) and EPS (EPS$_{pr}$) was measured by the Lowry method (Lowry et al., 1951). The concentration of polysaccharide in SMP (SMP$_{ps}$) and EPS (EPS$_{ps}$) was determined by the phenol-sulfuric method (DuBois et al., 1956). All analyses were conducted in duplicate and

their average values were reported.

2.4.2 ATP measurement

ATP content of the sludge was measured using the BacTiter-Glo (Promega Corporation) kit and protocol. The steps were as follows (Berney et al., 2008; Habermacher et al., 2015; Hammes et al., 2010). Firstly, 100 μL of suspended sludge sample was mixed with 100 μL of reagent. Secondly, the fouling layer was scraped carefully from the membrane surface by a glass stick at the end of the operation, then re-suspended with ultrapure water and homogenized. Thirdly, the reaction was carried out at 38 °C with 10 s incubation time on a vortex mixer. All samples were measured in duplicate.

2.4.3 Particle size

The cultured sludge was collected immediately after 24 hours. The particle size distribution (PSD) of the activated sludge was estimated using a Malvern Mastersizer 2000 instrument.

2.4.4 EEM analyses

EEM fluorescence spectroscopy was utilized to characterize SMP of the mixed liquor sludge, and the method was described by Meng et al. (Meng et al., 2011). Excitation and emission spectra were scanned from 220 to 450 nm in 5 nm increments and from 250 to 550 nm in 1 nm increments, respectively.

2.4.5 Other methods

Spectrophotometric measurements of DNP solutions were conducted using a UV-vis spectrophotometer (UV-2550, Shimadzu) in the 190-700 nm wavelength range.

3. Results and discussion

3.1 Effect of DNP on membrane fouling potential

3.1.1 Flux decline

In order to understand the membrane fouling potential by adding DNP, short-term dead-

end ultrafiltration tests were performed. As seen in Fig. 1(a), the curve of the permeate flux dropped dramatically in S2, and the specific flux was down to 0.1 at the end of the filtration. The least severe flux decline occurred in S4, and the control system (S1) came in second place. It can be concluded that the addition of DNP influenced the fouling rate of ultrafiltration membrane. High dosage (45 mg/g VSS) alleviated membrane fouling efficiently, whereas low dosage (15-30 mg/g VSS) accelerated the fouling rate. Similarly, Xu and Liu (2011) found that the addition of 33.3 mg DNP/g VSS reduced fouling resistance of nylon membranes. However, they did not explore the phenomenon of membrane fouling under low DNP concentration. The possible reasons for the potential fouling mechanisms will be discussed in more detail in Section 4.

3.1.2 Filtration resistance analyses

To comprehend the flux decline results, the distribution of the filtration resistance was analyzed. The total filtration resistance consisted of the resistances of the membrane, pore blocking and cake layer. The total filtration resistance of the four samples was 12.0×10^{11} m^{-1}, 91.1×10^{11} m^{-1}, 21.3×10^{11} m^{-1} and 6.1×10^{11} m^{-1}, respectively, which is in line with the results of flux decline. More specifically, membrane resistance of all the groups was nearly the same with the value of around 2.5×10^{11} m^{-1}. The cake layer resistance in each case was 9.0×10^{11} m^{-1}, 87.5×10^{11} m^{-1}, 18.3×10^{11} m^{-1} and 3.3×10^{11} m^{-1}, which suggests that the cake layer resistance firstly increased and then decreased according to the DNP dosage. Low dosage would also increase the resistance of pore blocking, and high dosage led to a relative low resistance. Furthermore, it can be calculated that the cake layer resistance occupied large proportions (54%-96%) of the total filtration resistance. Hence, cake layer resistance was the dominant form of total resistance for all samples. The conclusion can be drawn that low dosage of DNP aggravated cake layer fouling, while high dosage of DNP significantly retarded the cake layer fouling. However, the proportions of pore blocking resistance increased instead.

3.1.3 Fouling model analyses

In addition, classic filtration models were applied to better understand the influence of adding DNP on membrane fouling. The simple regression results of the four models are summarized in Table 1. The R^2 values were higher than 0.99 under the models of standard blocking, intermediate blocking and cake filtration in S1, which suggested that the fouling model of S1 was a combination of all three types. It is can be seen that the primary fouling model of S2 was cake filtration, which agrees with the results of resistance distribution. The fouling model might fall between standard blocking and intermediate blocking in S3. With regard to S4, the R^2 value was 0.999 under the model for standard blocking. Therefore, although low dosage of DNP led to a model of cake layer filtration, high dosage resulted in standard or intermediate pore blocking. We further analyzed the fouling mechanisms in Section 4.

Fig. 1

3.2 Effect of adding DNP on sludge reduction

3.2.1 Sludge yield

It is well known that energy uncoupling can inhibit the growth of activated sludge (Low & Chase, 1998). In the current study, the addition of DNP indeed reduced sludge concentration after 24 hours. As shown in Fig. 2(a), the VSS concentrations of the four groups were 1.98 g/L, 1.53 g/L, 1.4 g/L and 1.25 g/L, respectively. Sludge reduction reached the maximum of 37.5% when the dosage of 45 mg/g VSS was employed. Low and Chase (1998) found that biomass production efficiency declined by 62% when the feed was supplemented with 100 mg/L p-nitrophenol (pNP); there was a simultaneous increase in the specific substrate uptake rate. Li et al. (2012) added TCS as a metabolic uncoupler to the sludge, and the sludge reduction rate was able to reach 50%. Therefore, our results are consistent with the literature wherein DNP (as a metabolic uncoupler) could reduce the mass of sludge efficiently.

3.2.2 ATP content

ATP contents of the sludge samples were tested immediately after 24 hours culturing by DNP. It can be seen that ATP content decreased when the dosage of DNP increased. The lowest value was 18.6 umol/gVSS, which was observed under the dosage of 45 mg DNP/gVSS (Fig. 2b). Consequently, the addition of DNP restrained the synthesis of ATP. Xu and Liu (2011) found that cellular ATP content deceased with exposure to DNP, and ATP content fell further with the exposure time. Jiang and Liu (2013) proved that TCS was used to inhibit ATP synthesis, thus leading to the breakup of the aerobic granular sludge. In the current study, we mainly explored the effect of energy uncoupling on the sludge and the performance of the membrane filtration during the initial stage, which can guide the long-term MBR process. It can be speculated that the optimum dosage of DNP might be even lower in a real long-term MBR process.

Fig. 2

3.2.3 Particle size distribution

Fig. 3 illustrates the particle size distribution of sludge samples, which were already cultured for 24 hours by DNP addition. There were two main peaks in each sample. The position of the peaks moved left in the samples with added DNP compared with the control. The average particle sizes of the four samples were 189 μm, 115 μm, 84 μm and 68 μm, respectively. The addition of DNP reduced the average size of the sludge compared with the control, and the peak value also decreased with an increasing DNP concentration. The reduced particle size might be associated with the reduction of sludge concentration. Jiang and Liu (2013) reported that adding TCS could dramatically decrease the mean size (from 950 μm to 300 μm) and density (from 1.025 to 1.005 g/ml), which is consistent with our results that the chemical uncouplers broke up the sludge floc.

Fig. 3

3.3 Effect of DNP on sludge properties

In order to recognize the main reason for the fouling tendency of different samples, the properties of activated sludge, namely, SMP of the mixed liquor and EPS contents of the sludge, were systematically quantified following the addition of DNP under different dosages.

3.3.1 SMP and EPS contents

It is widely reported that EPS and SMP of sludge play crucial roles in MBRs' experience of membrane fouling (Drews, 2010; Meng et al., 2009). Fig. 4(a) presents the EPS content of the four samples. The EPS_{pr} contents of these four samples were 86.6 mg/gVSS, 65.3 mg/gVSS, 50.2 mg/gVSS and 43.9 mg/gVSS, respectively. Meanwhile, EPS_{ps} contents of the four samples also revealed a downward trend (from 62.7 mg/gVSS down to 31.6 mg/gVSS). As a consequence, the addition of DNP reduced the EPS contents (including polysaccharides and proteins) of the mixed sludge compared with the control, and high dosage resulted in relatively low EPS contents. Similarly, Jiang and Liu (2010) reported that the addition of 4 mg/L TCS could significantly inhibit the production of extracellular proteins, but only minimally affect extracellular polysaccharides in the aerobic granular sludge system.

In contrast, the concentrations of SMP of the mixed sludge increased with the dosage of DNP in Fig. 4(b). Both the dissolved polysaccharides and proteins increased from 3.2 mg/L to 15.7mg/L and from 4.8 mg/L to 21.1 mg/L with the increased dosage, respectively. Li et al. (2012) found that the addition of TCS in the activated sludge system led to more production of SMP, especially proteins, and the contents of both polysaccharides and proteins increased with substrate degradation. Indicated here is that the formation of SMP had a close relationship with substrate metabolism and utilization. Li et al. (2012) also pointed out that a high concentration of TCS led to equally high SMP production, and the sludge released more SMP with more

exposure time.

As well, the dissolved polysaccharides and proteins in the permeates were quantified. As shown in Fig. 4(c), the concentrations of dissolved polysaccharides and proteins increased with the DNP dosage, and this tendency was similar to the results concerning SMP of the mixed sludge. These findings revealed that large proportions of the molecular weight of dissolved SMP were smaller than membrane pores, and the ultrafiltration membrane did not sufficiently retain the dissolved polysaccharides and proteins released by the stimulation of added DNP.

Fig. 4

3.3.2 EEM analyses

The fluorescence spectra data are illustrated in Fig. 5. Four major peaks identified from the fluorescence spectra of SMP samples are evident in the literature. The peaks were observed at excitation/emission wavelengths (Ex/Em) of 235-240/340-355 nm, 275-280/320-330 nm, 240-260/390-445 nm and 290-350/410-435 nm representing aromatic proteins, trypto tryptophan protein-like substances, fulvic-like substances and humic acid-like fluorophores (Ding et al., 2014). It can be seen that four main peaks were visible only in S1, yet there was no peak in the other three samples. These phenomena disagree with the conclusions above that DNP led to the release of SMP. In order to explain this, pure solutions of DNP were detected by UV-vis. All the DNP samples demonstrated extended absorption in the visible light region at 300-450 nm (see Fig. S1), which indicated that the presence of DNP in the samples indeed disturbed the fluorescent organics' absorbance. Thus there were no peaks in S2, S3 and S4. It should be noted that fluorescence EEM could not predict membrane fouling when DNP existed.

Fig. 5

3.4. Mechanisms of membrane fouling

As shown above, the addition of metabolic uncouplers (DNP) changed several properties

of the activated sludge. It is interesting to note that the trends in membrane fouling varied quite significantly from each other. We will discuss the potential reasons in more detail below.

3.4.1 High dosage of DNP retarded membrane fouling

The results above revealed that the addition of DNP reduced the sludge's mass, and could break the sludge floc into small pieces. It also shows that the activated sludge released intracellular organic matter such as proteins and polysaccharides. As well, ATP contents were reduced with a larger dosage, which also led to changes in the EPS contents. Usually, the synthesis of proteins, polysaccharides and lipids requires 36.4 mmolATP/g, 12.6 mmolATP/g and 2 mmolATP/g, respectively (Russell, 2007). The reduced ATP content thus resulted EPS contents decreasing in the sludge. The fouling model analyses indicated that membrane fouling was due to the combined effects of standard pore blocking, intermediate blocking and cake filtration in the control system (without any chemical uncouplers). In general, the initial fouling in MBR systems is pore blocking due to the small molecular weight compounds, followed by cake layer formation owing to: firstly, the large molecular weight organics; and secondly, bacteria cells attached to the membrane surface. Several studies of filtration models revealed that the fouling of UF and MF membranes was characterized by the initial pore blocking mechanism transitioning to cake filtration at a later phase of filtration (Lee et al., 2013; Yuan et al., 2002).

However, the fouling model was standard blocking in the high DNP context. This can be explained as follows. Firstly, the sludge particles decreased the most compared with the others (see Section 3.2.3, Fig. 3), which might aggravate pore blocking. Secondly, low dosage caused the disassembly of the sludge floc, and the sludge released intracellular proteins and polysaccharides into the bulk solution. These processes confirmed the statement above and the released low molecular weight organics caused standard blocking. This can be proved by the quantification of the permeate whereby more proteins and polysaccharides were present in the

high dosage scenario when compared to the other samples. Thirdly, EPS contents including the proteins and polysaccharides decreased dramatically. EPS have been reported not only as major sludge floc components keeping the floc in a three-dimensional matrix, but also as key membrane foulants in MBR systems (Meng et al., 2009). Sludge cells deposited on the membrane surface by the presence of EPS (acted as a glue), and formed a dense cake layer. However, the bio-cake layer was difficult to form on the membrane due to the low EPS contents in the high DNP sample, which agreed with the analyses of the fouling model. In essence, adding a high dose of DNP to the sludge retarded the cake layer fouling and postponed the cake layer formation in the MBR's initial filtration stage. Based on our understanding of the results, a schematic illustration of the proposed DNP addition to membrane bio-fouling is shown in Fig. 6.

Fig. 6

3.4.2 Low dosage of DNP accelerated membrane fouling

Although the addition of DNP reduced sludge concentration and EPS contents, the results of the membrane fouling were opposite to the phenomenon of high dosage. The analyses of fouling model indicated that low dosage of DNP led to severe cake layer fouling.

In the first case, sludge particles reduced by the addition of DNP as stated above, and the small particles and colloids might increase the problem of cake fouling in the MBR. The sludge particle size was always significantly correlated inversely to the membrane fouling resistance (Meng et al., 2006). Secondly, the concentration of SMP released from the mixed sludge increased with the dosage. As stated in Section 4.1, the released SMP from the mixed sludge were low molecular weight organics able to pass through the membrane. However, it can be calculated that the penetration rates of the four groups were 40.8%, 29.3%, 20.3% and 16.0%, respectively (Section 3.3.1, Fig. 4). It is revealed that larger proportions of organics were retained by the membrane in the case of low DNP, and these colloidal proteins and

polysaccharides may contribute to the gel layer adhered on the membrane surface. This is one of the key reasons for the high resistance of cake layer filtration. Thirdly, although the EPS contents of the mixed sludge declined in the case of low DNP, the reduced level was not as high as the case of high DNP (see Fig. 4a). In other words, large amounts of EPS were still present in the mixed liquor, acting as a glue that might combine the bacteria, colloids and dissolved SMP tightly on the membrane surface. High content of EPS secreted by microorganisms always leading to a severe fouling (Hao et al., 2016; Sweity et al., 2011; Xu et al., 2014). This was comparable to the case regarding high dosage of DNP. As seen in Fig. 6, the dense bio-cake layer formed by the EPS was another key reason for the occurrence of serious membrane fouling (especially for cake layer fouling) under the low DNP scenario. Furthermore, low dosage of DNP accelerated the transition rate of the fouling model from pore blocking to cake layer filtration in comparison with the control sample.

4. Conclusion

The effects of energy uncoupling (DNP addition) on bio-fouling potential of MBRs were investigated. Low dosage caused more serious membrane fouling, whereas high dosage alleviated fouling compared with the control. Low DNP resulted in a small particle size and large amount of SMP being retained on the membrane surface and subsequently forming a dense fouling layer. This in turn increased the cake layer resistance. Although SMP concentrations were even higher in the case of high DNP, EPS were strongly inhibited instead. The bio-cake did not develop on the membrane and consequently retarded cake layer resistance. Finally, this study has provided a useful and practical fouling control strategy for the MBR process.

Acknowledgements

References

Adav, S.S., Lee, D.J. 2008. Extraction of extracellular polymeric substances from aerobic granule with compact interior structure. *Journal of Hazardous Materials*, **154**(1-3), 1120-1126.

Berney, M., Vital, M., Hülshoff, I., Weilenmann, H.-U., Egli, T., Hammes, F. 2008. Rapid, cultivation-independent assessment of microbial viability in drinking water. *Water Research*, **42**(14), 4010-4018.

Ding, A., Liang, H., Qu, F., Bai, L., Li, G., Ngo, H.H., Guo, W. 2014. Effect of granular activated carbon addition on the effluent properties and fouling potentials of membrane-coupled expanded granular sludge bed process. *Bioresource Technology*, **171**(1), 240-246.

Ding, A., Pronk, W., Qu, F., Ma, J., Li, G., Li, K., Liang, H. 2015. Effect of calcium addition on sludge properties and membrane fouling potential of the membrane-coupled expanded granular sludge bed process. *Journal of Membrane Science*, **489**, 55-63.

Drews, A. 2010. Membrane fouling in membrane bioreactors—Characterisation, contradictions, cause and cures. *Journal of Membrane Science*, **363**(1-2), 1-28.

DuBois, M., Gilles, K.A., Hamilton, J.K., Rebers, P.A., Smith, F. 1956. Colorimetric Method for Determination of Sugars and Related Substances. *Analytical Chemistry*, **28**(3), 350-356.

Habermacher, J., Benetti, A.D., Derlon, N., Morgenroth, E. 2015. The effect of different aeration conditions in activated sludge – Side-stream system on sludge production, sludge degradation rates, active biomass and extracellular polymeric substances. *Water Research*, **85**, 46-56.

Hammes, F., Goldschmidt, F., Vital, M., Wang, Y., Egli, T. 2010. Measurement and interpretation of microbial adenosine tri-phosphate (ATP) in aquatic environments. *Water Research*, **44**(13), 3915-3923.

Hao, L., Liss, S.N., Liao, B.Q. 2016. Influence of COD:N ratio on sludge properties and their role in membrane fouling of a submerged membrane bioreactor. *Water Research*, **89**, 132-141.

Jiang, B., Liu, Y. 2013. Dependence of structure stability and integrity of aerobic granules on ATP and cell communication. *Appl Microbiol Biotechnol*, **97**(11), 5105-12.

Jiang, B., Liu, Y. 2010. Energy uncoupling inhibits aerobic granulation. *Appl Microbiol Biotechnol*, **85**(3), 589-95.

Lee, S.-J., Dilaver, M., Park, P.-K., Kim, J.-H. 2013. Comparative analysis of fouling characteristics of ceramic and polymeric microfiltration membranes using filtration models. *Journal of Membrane Science*, **432**, 97-105.

Li, Y., Li, A.M., Xu, J., Liu, B., Fu, L.C., Li, W.W., Yu, H.Q. 2012. SMP production by activated sludge in the presence of a metabolic uncoupler, 3,3',4',5-tetrachlorosalicylanilide (TCS). *Appl Microbiol Biotechnol*, **95**(5), 1313-21.

Lin, H., Zhang, M., Wang, F., Meng, F., Liao, B.-Q., Hong, H., Chen, J., Gao, W. 2014. A critical review of extracellular polymeric substances (EPSs) in membrane bioreactors: Characteristics, roles in membrane fouling and control strategies. *Journal of Membrane Science*, **460**, 110-125.

Liu, Y. 2000. Effect of chemical uncoupler on the observed growth yield in batch culture of activated sludge. *Water Research*, **34**(7), 2025-2030.

Low, E.W., Chase, H.A. 1998. The use of chemical uncouplers for reducing biomass production during biodegradation. *Water Science and Technology*, **37**(4), 399-402.

Lowry, O.H., Rosebrough, N.J., Farr, A.L., Randall, R.J. 1951. PROTEIN MEASUREMENT WITH THE FOLIN PHENOL REAGENT. *Journal of Biological Chemistry*, **193**(1), 265-275.

Malaeb, L., Le-Clech, P., Vrouwenvelder, J.S., Ayoub, G.M., Saikaly, P.E. 2013. Do biological-based strategies hold promise to biofouling control in MBRs? *Water Res*, **47**(15), 5447-63.

Meng, F., Chae, S.R., Drews, A., Kraume, M., Shin, H.S., Yang, F. 2009. Recent advances in membrane bioreactors (MBRs): membrane fouling and membrane material. *Water Res*, **43**(6), 1489-512.

Meng, F., Zhang, H., Yang, F., Zhang, S., Li, Y., Zhang, X. 2006. Identification of activated sludge properties affecting membrane fouling in submerged membrane bioreactors. *Separation and Purification Technology*, **51**(1), 95-103.

Meng, F., Zhang, S., Oh, Y., Zhou, Z., Shin, H.S., Chae, S.R. 2017. Fouling in membrane bioreactors: An updated review. *Water Res*, **114**, 151-180.

Meng, F., Zhou, Z., Ni, B.J., Zheng, X., Huang, G., Jia, X., Li, S., Xiong, Y., Kraume, M. 2011. Characterization of the size-fractionated biomacromolecules: tracking their role and fate in a membrane bioreactor. *Water Res*, **45**(15), 4661-71.

Russell, J.B. 2007. The energy spilling reactions of bacteria and other organisms. *Journal of Molecular Microbiology and Biotechnology*, **13**(1-3), 1-11.

Shen, Y., Zhao, W., Xiao, K., Huang, X. 2010. A systematic insight into fouling propensity of soluble microbial products in membrane bioreactors based on hydrophobic interaction and size exclusion. *Journal of Membrane Science*, **346**(1), 187-193.

Sweity, A., Ying, W., Ali-Shtayeh, M.S., Yang, F., Bick, A., Oron, G., Herzberg, M. 2011. Relation between EPS adherence, viscoelastic properties, and MBR operation: Biofouling study with QCM-D. *Water Research*,

45(19), 6430-6440.

Wang, Q., Wang, Z., Zhu, C., Mei, X., Wu, Z. 2013. Assessment of SMP fouling by foulant–membrane interaction energy analysis. *Journal of Membrane Science*, **446**,154-163.

Xiong, Y., Liu, Y. 2010. Involvement of ATP and autoinducer-2 in aerobic granulation. *Biotechnol Bioeng*, **105**(1), 51-8.

Xu, H., Liu, Y. 2011. Control and cleaning of membrane biofouling by energy uncoupling and cellular communication. *Environmental Science and Technology*, **45**(2), 595-601.

Xu, M., Bernards, M., Hu, Z. 2014. Algae-facilitated chemical phosphorus removal during high-density Chlorella emersonii cultivation in a membrane bioreactor. *Bioresource Technology*, **153**, 383-387.

Yuan, W., Kocic, A., Zydney, A.L. 2002. Analysis of humic acid fouling during microfiltration using a pore blockage–cake filtration model. *Journal of Membrane Science*, **198**(1), 51-62.

Zhou, Z., Meng, F., He, X., Chae, S.-R., An, Y., Jia, X. 2015. Metaproteomic Analysis of Biocake Proteins To Understand Membrane Fouling in a Submerged Membrane Bioreactor. *Environmental Science & Technology*, **49**(2), 1068-1077.

Fig. 1 DNP addition on membrane fouling potential: (a) normalized flux decline of ultrafiltration membrane; (b) filtration resistance distribution

Fig. 2 Effect of DNP concentration on sludge reduction: (a) sludge yield; (b) ATP content

Fig.3 Effect of DNP addition on particle size of the sludge

Fig. 4 Effect of DNP addition on the EPS and SMP concentrations: (a) EPS contents; (b) SMP concentration of the mixed sludge; (c) SMP concentration of the permeates

Fig. 5 Effect of DNP addition on the EEM fluorescence spectra of SMP. where, S1: control; S2: 15 mg DNP /g VSS; S3: 30 mg DNP /g VSS; S4: 45 mg DNP /g VSS

Fig. 6 Schematic illustration of the influence of DNP addition on the membrane fouling

Tables

Table 1 Fitting the curves of flux decline: (1) complete blocking; (2) standard blocking; (3) intermediate blocking; (4) cake filtration.

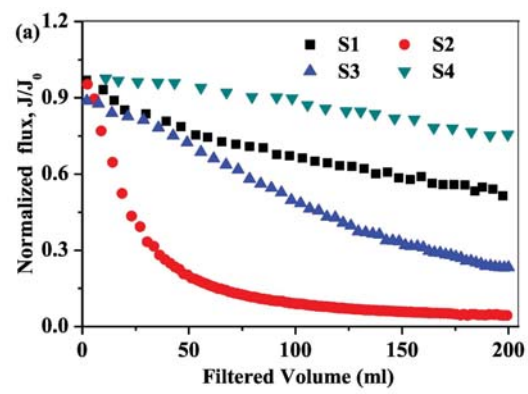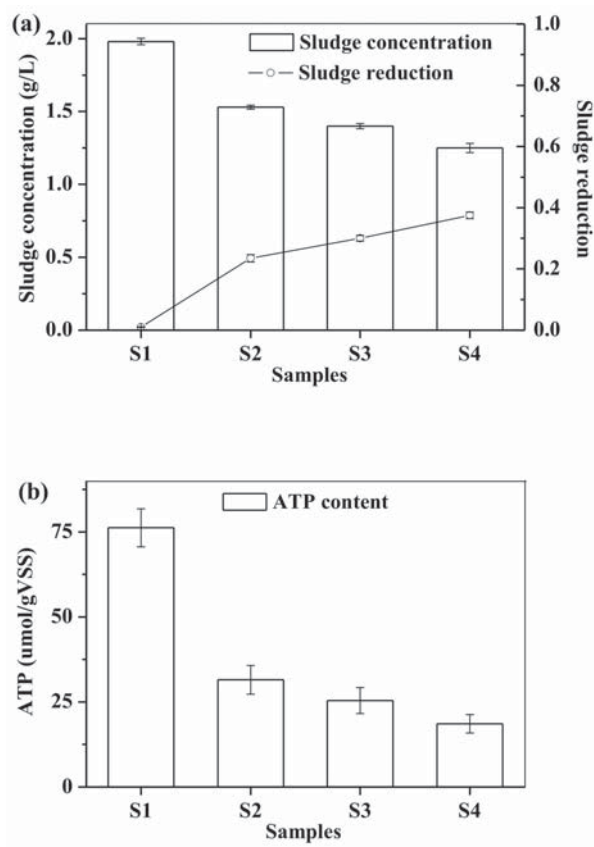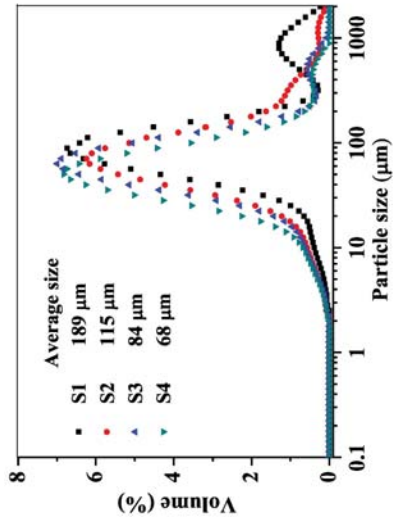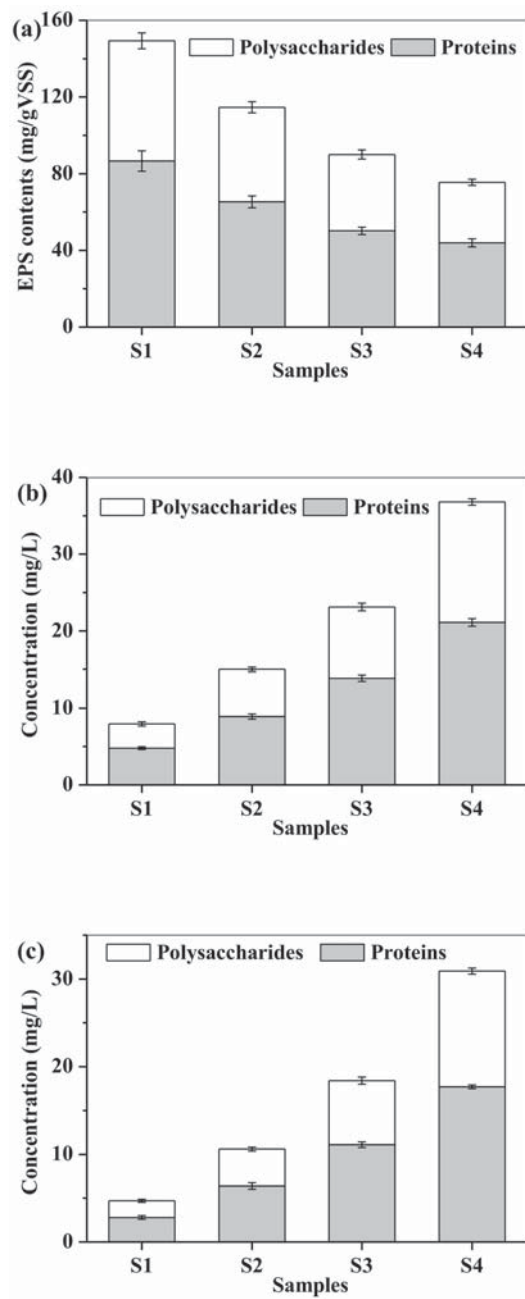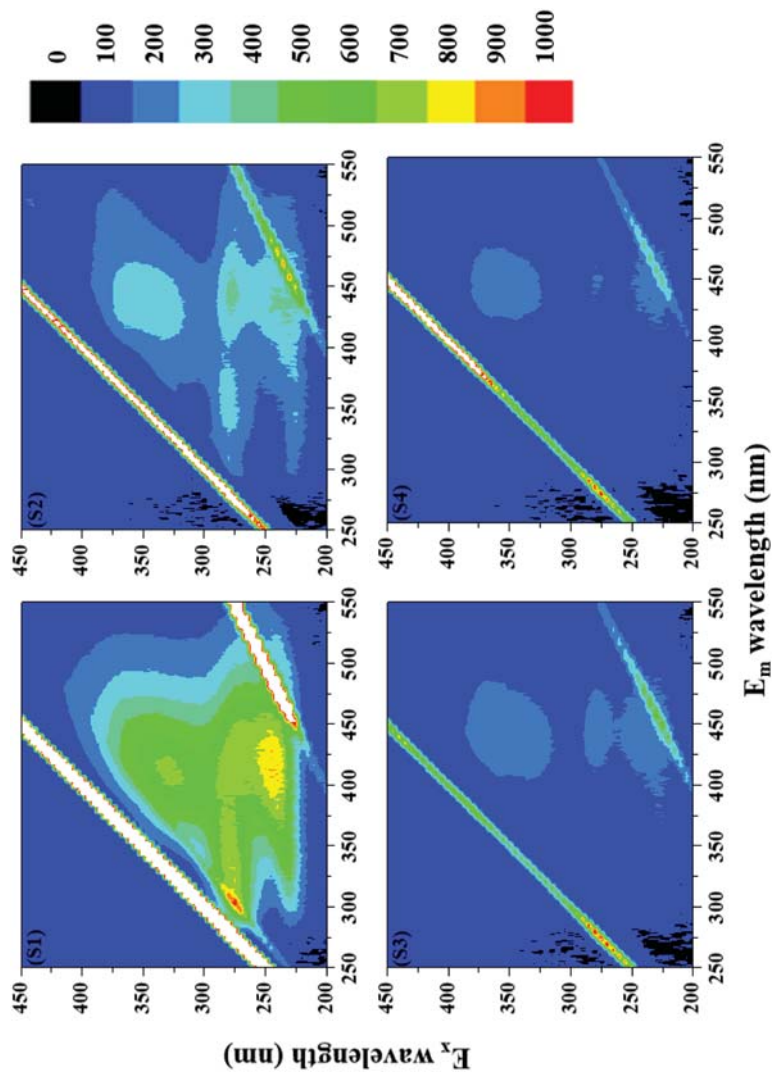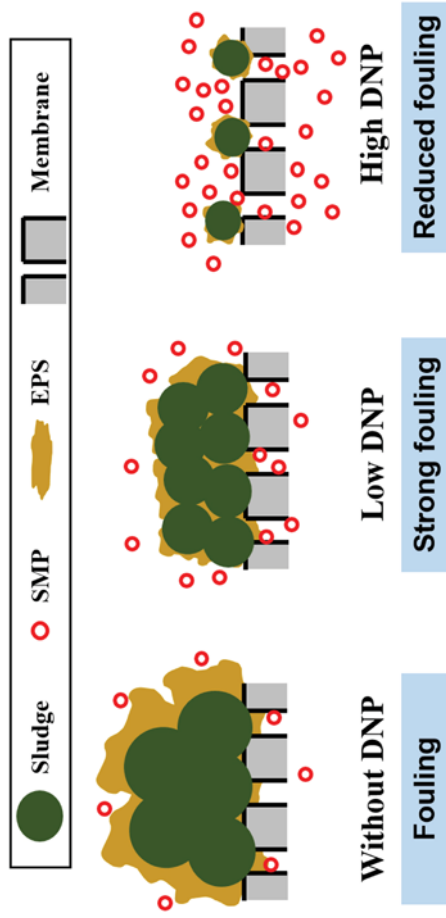| Sample	R^2 valu			
	Complete blocking	Standard blocking	Intermediate blocking	Cake filtration
S1	0.987	*0.997*	*0.995*	*0.993*
S2	0.497	0.984	0.881	*0.996*
S3	0.981	*0.991*	*0.994*	0.952
S4	0.956	*0.999*	0.965	0.976
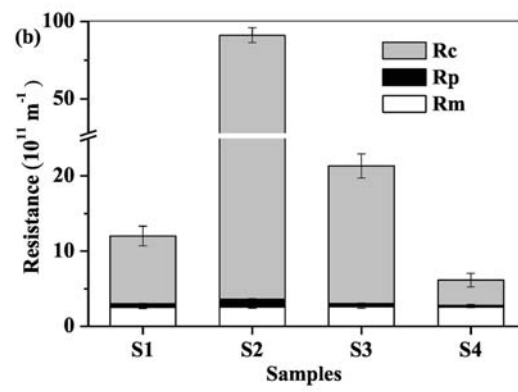
Figure 1

Figure 2

Figure 3

Figure 4

Figure 5

Figure 6